

FIRB SOLENOID PACKAGE IN CRYOMODULE AND LOCAL MAGNETIC SHIELD*

K. Saito[†], H. Ao, B. Bird, R. Bliton, N. Bultman, F. Casagrande, C. Compton, J. Curtin, K. Elliott, A. Ganshyn, W. Hartung, L. Hodges, K. Holland, S-H Kim, S. Lidia, D. Luo, S. Miller, D. Morris, L. Nguyen, D. Norton, J. Popielarski, L. Popielarski, T. Russo, J. Schwartz, S. Shanab, M. Shuptar,

D. Victory, C. Wei, J. Wei, M. Xu, T. Xu, Y. Yamazaki, C. Zhang, Q. Zhao

Facility for Rare Isotope Beams, Michigan State University, East Lansing, MI, USA

A. Facco, INFN – Laboratori Nazionali di Legnaro, Legnaro (Padova), Italy

K. Hosoyama, M. Masuzawa, High Energy Accelerator Research Organisation, Tsukuba, Japan

R. Laxdal, TRIUMF, Vancouver, BC, Canada

Abstract

FIRB cryomodule design has a feature: solenoid package(s) and local magnetic shields in the cryomodule. In this design, exposing SRF cavities to a very strong fringe field from the solenoid is concerned. A tangled issue between solenoid package design and magnetic shield one has to be resolved. FIRB made intensive studies, designed, prototyped, validated the solenoid packages and magnetic shields, and finally certified them in the bunker test. This paper reports the activity results, and LS1 commission-ing results in FIRB tunnel. This is a FIRB success story.

FEATURE OF FIRB CRYOMODULE DESIGN AND CONCERNS

FIRB cryomodule design has a feature: 8 T superconducting solenoid package(s) in the cryomodule [1]. This is to have frequent strong focussing heavy ion beams with a high space efficiency. One example of the FIRB cryomodules is shown in Fig. 1 for $\beta=0.041$ quarter wave resonators (QWRs). The original solenoid field design was 9 T but it is so critical for NbTi superconducting wire at 4.5 K operation, which was pointed out in the cryomodule workshop at MSU [2]. As illustrated in Fig. 2, FIRB beam optics was revised from the constant beta lattice (9 T) scheme to the constant beam size optics (8 T) in order to mitigate this issue. The solenoid design field was reduced to 8 T by this new optics.

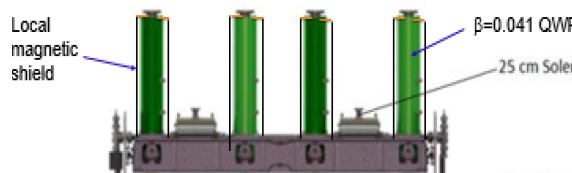


Figure 1: FIRB cryomodule design example for 0.041 QWR coldmass. Two SC magnet packages and local magnetic shield around cavity are seen.

Another concern in this cryomodule design is to expose SRF cavities to a strong fringe field from the solenoid

pachage. When cavity quenched, serious Q-drop could happen by the flux trapping. FIRB employs the local magnetic shield close to the cavity in order to mitigate this problem as shown in Figs. 1 and 3. This scheme can also reduce the shield material cost. However, what the remnant field strength in the shield produces how much Q-drop at cavity quench was unknown. We needed the information to make the FIRB shield design and solenoid design.

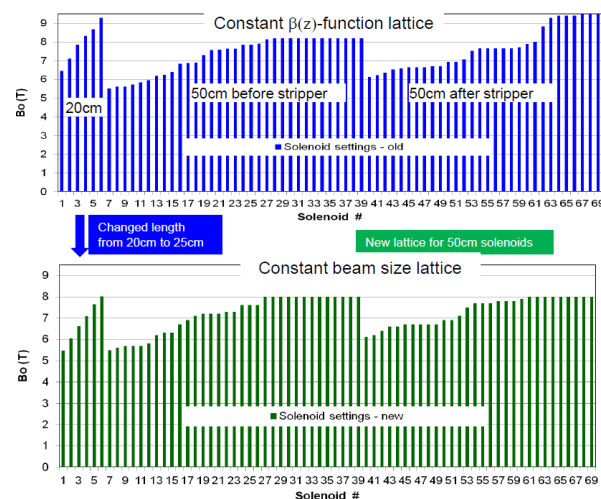


Figure 2: FIRB beam ophitic change from the constant beta scheme to constant beam size, which reduces the solenoid field from 9 T to 8 T.

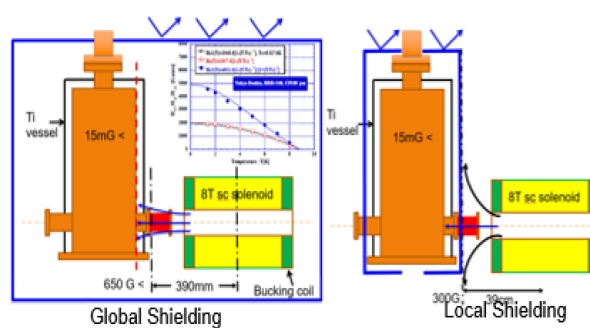


Figure 3: Cavity fringe field exposure during solenoid operation, left (Blue Square) is the global magnetic shied and right local shield (blue square).

* Work supported by the U.S. Department of Energy Office Science of under Cooperative Agreement DE-S0000661 and the National Science Foundation under Cooperative Agreement PHY-1102511

[†] Saito@frib.msu.edu

Q-DROP AT CAVITY QUENCH DUE TO FLUX TRAPPING

One $\beta=0.53$ (322MHz) half-wave resonator (HWR) was quench tested energizing a superconducting solenoid close to the short area of the cavity as seen in Fig. 4 top. The solenoid fringe field was measured on the short area of the cavity. The cavity was quenched under a solenoid fringe field, then measured the Q-drop still under the field, and measured Q_0 switching off the solenoid. This procedure was repeated from 2.5 G to 50 G (Fig. 4 bottom). The residual Q-drop: Q_0 (before solenoid energizing) — Q_0 (after quench but solenoid switched off) is estimated about 10% degradation at 1 G (Fig. 4 bottom). This degree of degradation is manageable in the machine operation. So one criteria for solenoid/magnetic shield design was set that the remnant field in the magnetic shield by the penetrated fringe field through magnetic shield should be less than 1 G.

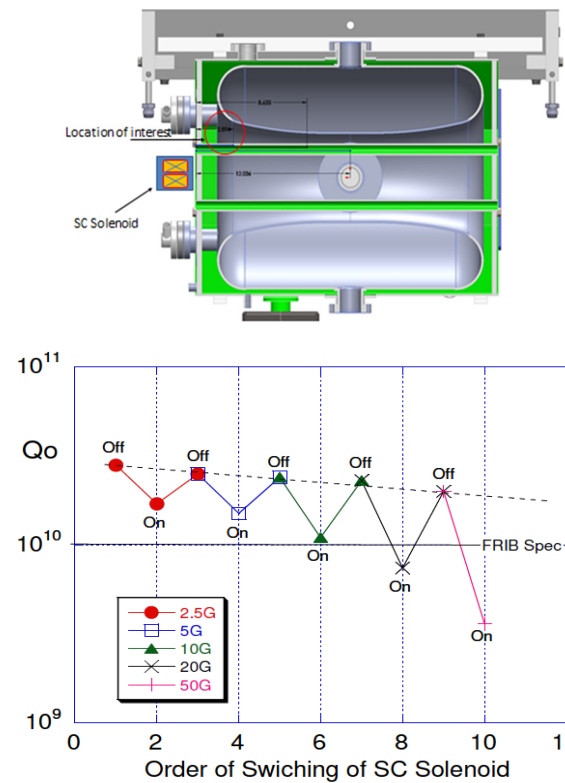


Figure 4: HWR cavity quench test operating solenoid. The cavity was quenched under a solenoid field and confirmed Q-drop (bottom).

FLUX PENETRATION INTO MAGNETIC SHIELD

For the solenoid design, we need to know the onset field of which the fringe field starts to penetrate remarkably into the magnetic shield. It was initially measured at a room temperature (RT) using a normal conducting solenoid, and then at 10 K using a superconducting solenoid [3]. The magnetic shield was made of A4K or Cryoperm. The fringe field was measured on the outer and inner surfaces of the

shield. The result is shown in Fig. 5. The onset penetration field is observed at around 390 G (RT) and 300 G (10 K). Here, the second criteria for the solenoid design was made clear: fringe field strength <300 G on the outer magnetic surface at cold.

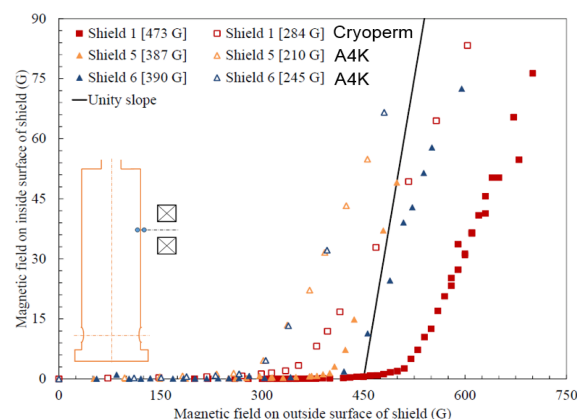


Figure 5: FRIB SRF cavity families with helium jacket.

FRIB SOLENOID PACKAGE DESIGN

FRIB needs two types of solenoid package: 25 cm packages for 0.041QWR CMs and 50 cm ones for 0.085QWR CMs, 0.29HWR CMs, and 0.53HWR CMs. Those packages consist of one solenoid and two sets of dipoles for beam steering. The specifications are listed in Table 1. The interface between the solenoid and the local magnetic shield had already fixed in the cryomodule design [1]. For instance, the distance between the 50 cm solenoid centre in longitudinal and the magnetic shield surface was 39 cm for the 0.53 HWR cryomodule. These solenoid packages were designed under the second criteria and the space configuration: fringe field <300 G on the magnetic shield. POASON and finally CST code were utilized to calculate magnetic field [4]. Bucking coils were employed at both solenoid ends to reduce the fringe field. Figure 6 shows the modelling of the solenoid package for CST. Figure 7 shows the 2D field distribution by POASON. We could successfully make the solenoid package design to meet the criteria. In this design, the maximum fringe field is 270 G at the magnetic shield 39 cm far from the solenoid centre (50 cm).

Table 1: FRIB Solenoid Package Specification

Packages	Maximum field on axis	Integrated field	Current
25 cm solenoid	8 T	13.87 T ² m	< 100 A
25 cm dipoles	0.12 T	0.03 Tm	< 20 A
50 cm solenoid	8 T	28.48 T ² m	< 100 A
50 cm dipoles	0.12 T	0.06 Tm	< 20 A
Aperture		40 mm for both solenoids	
Error between mechanical centre and field centre			< 0.3 mm

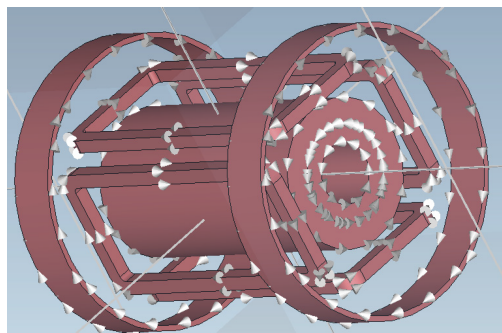


Figure 6: 50 cm solenoid package modelling for CST.

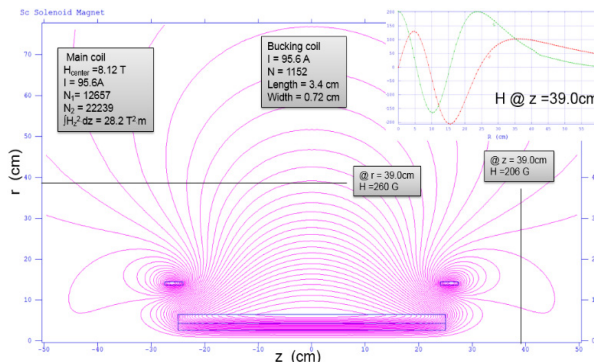


Figure 7: 2D field distribution by POASSON code.

SOLENOID PACKAGE PROTOTYPING

Based on the design, solenoid packages were successfully prototyped and cold tested at KEK for 25 cm package (just one piece) and at FRIB for 50 cm ones (four pieces). KEK applied dry winding based on their solenoid production experience, while MSU applied wet winding with Stycast based on their experience (Fig. 8). For the quench protection, KEK employed stainless coils, while MSU utilized diodes. Figure 9 (left) shows the 50 cm solenoid coldmass with diodes and the right is the package completed at MSU. The detail report of MSU prototyping is in the reference [4].



Figure 8: Solenoid winding, dry winding at KEK (left), and wet winding at MSU (right).

These solenoids were successfully validated the performance at both KEK (25 cm package) and MSU (50 cm packages). The result of 25 cm solenoid package cold test is reported in the reference [5, 6]. The result of 50 cm ones is in the reference [4].

FRIB ordered nine 25 cm solenoid packages and seventy-two 50 cm ones including spares to a solenoid production vendor. They successfully produced the packages based on

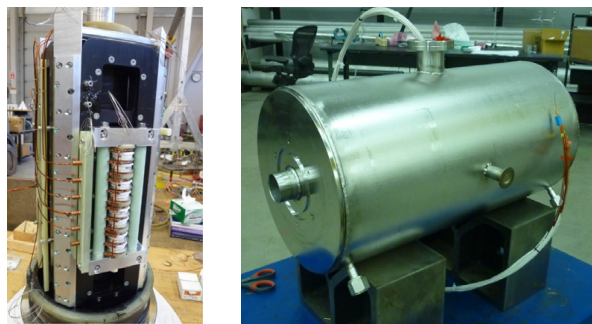


Figure 9: 50 cm solenoid package coldmass (left) with the stacked diodes for quench protection. A completed 50 cm solenoid package at MSU with dressed stainless helium jacket (right).

our designs. Before delivery, they made on-site cold test at 4 K, measured field distribution and the machine/field centre error (< 0.3 mm) at cold for every solenoid package. Solenoid quench happened in the vendor cold test at the frequency of 30% with 25 cm packages and 15% with 50 cm ones, however any quench happened in the bunker tests at FRIB.

LOCAL MAGNET SHIELD VALIDATION

As the next step, we needed to validate the local magnetic shield concept. The validation was carried out using the 0.085QWR development cryomodule and a 50 cm MSU prototyped superconducting solenoid package. One solenoid package was placed between two 0.085QWRs at one end of the cryomodule as seen in Fig. 10.



Figure 10: Coldmass on the cryomodule baseplate for the local magnetic shield design validation. Two cavities surrounded magnetic shield and one solenoid are seen.

The local magnetic shields were made of A4K. Flux gauges were located on the outer/inner shield surface. Two temperature sensors were put on the outer shield surface. During cool down the remnant field was 2.5 mG at the shield top-inside where the QWR is sensitive with the remnant field. It was 160 mG during the magnet operation: solenoid 8 T and dipoles 0.06 Tm. After degaussing, it decreased to 3.6 mG (FRIB goal < 15 mG). The shield temperature was 20–30 K during the cold test. Table 2 summarizes information of the field strength at top and bottom inside/outside

shield. The local shield concept was successfully validated for the 8 T solenoid package operation.

Table 2: Field Information at the Local Magnetic Shield Validation Test

Process	Shield TOP (mG)		Shield Bottom (mG)	
	Inside	Outside	Inside	Outside
After cool down (shield temp. 24.5K)	2.5	8.1	3.0	209.3
During SC solenoid package full operation (Solenoid 8 T, Dipoles 0.06 Tm)	-160.0	-358.2	-1636.5	-849.3
After solenoid package operation	30.1	26.4	14.6	290.6
After degaussing at 2K	3.6	7.6	-1.4	206.3

MAGNETIC SHIELD MATERIAL AND SHIELD DESIGN OPTIMIZATION

We found that the magnetic shield temperature is 20–30 K at CM cooled. KEK colleagues measured the permeability (μ) under external fields with several shield materials at 20 K (Fig. 11).

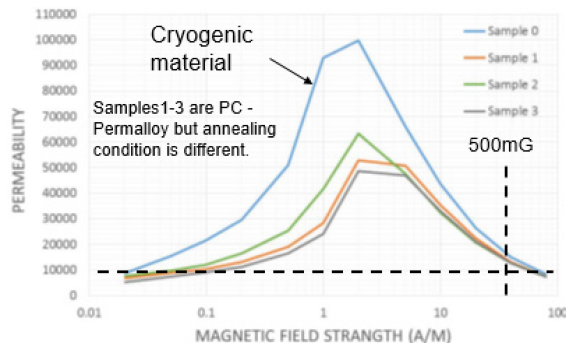


Figure 11: Field dependence of permeability at 20 K.

They compared cryogenic material (Cryoperm) and PC-Permalloy (a kind of conventional Mu-metal) and concluded that the benefit of μ in the cryogenic material is only 10–20% at 500 mG (Earth magnetic field). $\mu > 10000 @ 20$ K is available with PC-Permalloy.

Magnetic shield design was carefully optimized. Magnetic shield fabrication should be cost-effective for multi-cavities in one shield. Example is illustrated for 0.085QWR shield in Fig. 12. In this case, if no plate between cavities, μ needs 16000 to meet FRIB spec (15 mG), while adding a plate $\mu=9000$ meets the requirement. Similar optimization also took place for HWR cryomodules. Thus we confirmed that PC-Permalloy with $\mu > 9000$ is usable. We finally confirm this by validation test in the cryomodule as reported next. The FRIB magnetic shield specification is in Table 4.

MAGNETIC SHIELD VALIDATION

The magnetic shield design validation with Mu-metal was done using the FRIB first 0.085QWR production cryomodule (Fig. 13), which employs the magnetic shields design optimized. Both end cavities utilize single shield and other three cavities group uses one shield (multiple shield). In the



Figure 12: Example of magnetic shield optimization, 0.085 QWR CM case. If add plates between cavities, $\mu = 9000$ meets the FRIB requirement (< 15 mG in the shield).

mirror symmetry in Fig. 13, left side was used Mu-metal shields and right side utilized A4K shields.



Figure 13: FRIB first 0.085QWR production cryomodule. In the left (one cavity and other three cavities group) in the mirror symmetry PC Permalloy was used and right Mu-metal was used for magnetic shield material.

Table 3: Comparison of the Dynamic Load at 2 K Between Mu-metal and A4K Shields

Cavity	Dynamic load at bunker @ 5.6 MV/m [W]	Dynamic load at VTA @ 5.6 MV/m [W]	VTA Qo at 5.6 MV/m	Shield material
C#1	6.2	3.5	2.0 E+09	Mu-metal
C#2	2.4	3.2	2.2 E+09	Mu-metal
C#3	2.5	3.0	2.4 E+09	Mu-metal
C#4	1.0	2.9	2.7 E+09	Mu-metal
Total	12.1	12.6		
C#5	2.4	3.0	2.6E+09	A4K
C#6	2.5	2.7	2.9 E+09	A4K
C#7	2.4	2.7	2.9 E+09	A4K
C#8	2.6	2.6	2.7 E+09	A4K
Total	9.9	11.0		

Table 3 compares the 2 K cavity dynamic load in the bunker test between Mu-metal and A4K shields. The cavity performance in the VTA is also compared to the bunker test. In the bunker test Mu-metal shield looks worse in total cavity loss (12.1 W) comparing to that of the A4K shield (9.9 W), but it is due to the cavity performance. If compared the cavity loss between bunker test and VTA, both shields

have similar results to VTA test within measurement error 10–20%. As the conclusion, Mu-metal shield has similar cryogenic shield performance to the A4K material. Thus, we decided to employ the PC-Permalloy instead cryogenic material for all FRIB cryomodules except for 0.085QWR CMs, which was already ordered due to the long lead term delivery.

FRIB magnetic shield specification is summarized in Table 4. The $\mu > 9000$ specification looks tight but it is not true. The remnant magnetic shield was measured in the FRIB cryomodule vacuum chamber made of carbon steel and was 250 mG thanks to the shielding effect of the carbon steel. As seen in Fig. 10, the value of μ under the external field around 250 mG μ is > 20000 with PC-Permalloy, which brings a big margin for the shield performance.

Table 4: CFRIB Magnetic Shield Specification

CFRIB Magnetic Shield Specification	0.041QWR Cryomodule	HWR Cryomodule
Permeability	> 9000	> 9000
Thickness [mm]	1.00	2.00

FRIB SOLENOID BUNKER TEST

As date of mid-June 2019, FRIB has completed cryomodule bunker tests: four 0.041QWR CMs, eleven 0.085QWR CMs, twelve 0.29HWR CMs, and eight 0.53HWR CMs, which corresponds to 76% of the FRIB need. An example of the solenoid package bunker test (SCM509, $\beta=0.53$ 9th cryomodule) is shown in Fig. 14. The test consists of four

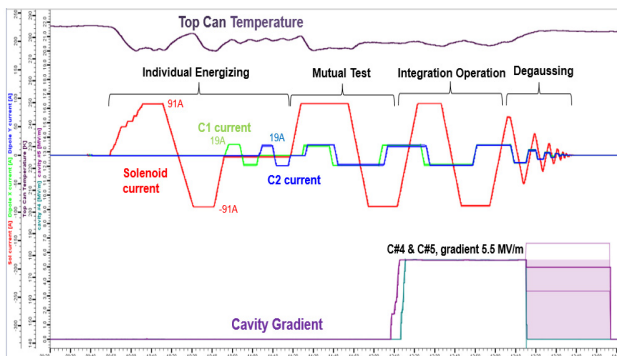


Figure 14: Solenoid package bunker test example (0.53HWR CM). All magnets were co-operated at the maximal field with cavities at operation field, all magnets were changed polarity. No quench happened. Solenoid package is very stable and robust.

steps: 1) energizing test for individual magnet, 2) mutual magnet operation test, 3) cavity/solenoid package integrated operation test, and 4) degaussing. In the individual magnet energizing test, magnets are excited up to the specification fields in sequentially: solenoid up to 91 A (> 8 T), dipoles up to 19 A ($> 0.03/0.06$ Tm). The polarity is also changed. In step 2), individual magnet is operated under the other magnet fields and checked the magnet frame robustness

against Lorentz forces from the other magnet fields. Step 3) is to investigate the potential flux trapping issue. When cavity operation faces unstable for example, multipacting, field emission or quench under the solenoid package fields, the cavity performance might be degraded by the flux trapping. In these test, any quenches happened with all solenoid packages.

Step 4 which is the end of solenoid package operation test is to degauss magnetized components by solenoid package operation. We control all components in FRIB cryomodules with magnetization. We concern the magnetization in random direction. We measure magnetization of all the components, and which are demagnetized using a degasser if observed magnetization. Components in the cryomodule should be not magnetized before the bunker test. The magnetization caused by solenoid package operation, it can be demagnetized by the degaussing cycle (amplitude is decreased by 25% in each cycle) of the solenoid package. Table 5 compares Q_0 between VTA and bunker tests. In any case the high Q performance is preserved in the bunker test.

Table 5: Q_0 Comparison Between VTA and Bunker Test

CM	Number of CMs tested	Q_0 FRIB-Spec	Q_0 Bunker test at Operation gradient	Q_0 VTA at Operation gradient
0.041	3 (4)	$1.2 \cdot 10^9$	$> 3.3 \pm 2.8 \cdot 10^9$	$5.7 \pm 0.7 \cdot 10^9$
0.085	11(11)	$1.8 \cdot 10^9$	$> 3.3 \pm 1.2 \cdot 10^9$	$4.0 \pm 1.0 \cdot 10^9$
0.29	12(12)	$5.5 \cdot 10^{10}$	$2.0 \pm 0.6 \cdot 10^{10}$	$1.4 \pm 0.2 \cdot 10^{10}$
0.53	18(8)	$7.6 \cdot 10^9$	$2.8 \pm 0.9 \cdot 10^{10}$	$1.9 \pm 0.4 \cdot 10^{10}$

LS1 COMMISSIONING

As date of February 2019, FRIB linac has been completed up to the first straight linac section (LS1) and 45°C bend (FS1b). This section installs three 0.041QWR CMs and eleven 0.085QWR CMs and one 0.085QWR matching CM. A 0.041QWR CM has two 25 cm solenoid packages, and a 0.085QWR CM has three 50 cm solenoid packages. The matching CM has no solenoid packages. In the LS1 commission we have operated these all solenoid packages: six 25 cm solenoid packages and thirty-three 50 cm ones.

During March 3–8, and April 8–12, all LS1 solenoid packages were tuned on and operated stably for long term. Solenoids were operated at current 20–64 A. Dipoles were operated < 5 A. All solenoids and dipoles were very stably operated. Any issues ascribed to these solenoid packages were not observed. The detail report is seen in the reference [7].

In this commission, ^{20}Ne , ^{40}Ar , ^{86}Kr and ^{129}Xe beams were successfully accelerated up to 20.3 MeV/u with 100% transmission. Beam centroid was tuned within ± 0.5 mm using on-line orbit response matrix based high-level applications. The highest current was 133euA peak, 3% duty cycle, average current of 4.0 euA, which corresponds to 31% of the design value.

SUMMARY

FRIB made many studies and validation tests to establish the cryomodule design: solenoid and local magnetic shield in the cryomodule. The design is successfully validated and proved to work well in the bunker test and beam commissioning.

REFERENCES

- [1] S. Miller, N. Bultman, A. Fox, M. Johnson, M. Leitner, T. Nellis, X. Rao, M. Shuptar, K. Witgen, Y. Xu, B. Bird, F. Casagrande, J. Ozelis, and R. Rose, “Low-Beta Cryomodule Design Optimized for Large-Scale Linac Installations”, in *Proc. SRF’13*, Paris, France, paper THOA04, pp. 825–829.
- [2] K. Hosoyama, “9T SC Solenoid Design, Fabrication and issues”, Workshop on Magnetic Shielding for Cryomodules, hosted by MSU March 6–7.
- [3] S. K. Chandrasekaran, K. Saito, S. Shanab, S. Chouhan, C. Compton, K. Elliot, M. Leitner, and J. Ozelis, “Magnetic Shield Material Characterization for the Facility for Rare Isotope Beam’s Cryomodules”, *IEEE Tran. On App. Supereon.*, vol. 25, no. 3, June 2015.
- [4] S. Shanab, K. Saito, K. Hosoyama, E. Burkhardt, Y. Yamazaki, S. Kenney, T. Weber, R. Witgen, R. Haas, E. Eicher, and J. VanAken, “Superconducting Solenoid Package Design, Fabrication, and Testing for FRIB”, *IEEE Trans. On App. Super.*, p. 4004404, March 2018.
- [5] K. Saito *et al.*, “SRF Developments at MSU for FRIB”, in *Proc. SRF’13*, Paris, France, Sep. 2013, paper MOP013, pp. 106–111.
- [6] K. Saito *et al.*, “Superconducting RF Development for FRIB at MSU”, in *Proc. LINAC’14*, Geneva, Switzerland, Aug.-Sep. 2014, paper THIOA02, pp. 790–794.
- [7] M. Xu *et al.*, “FRIB LS1 Cryomodule’s Solenoid Commissioning”, presented at the SRF’19, Dresden, Germany, Jun.-Jul. 2019, paper TUP089.